Applied Physics B (2018) 124:62
https://doi.org/10.1007/s00340-018-6932-y

Applied Physics B
Lasers and Optics

A broadband Tm/Ho-doped fiber laser tunable from 1.8 to 2.09 µm for intracavity absorption spectroscopy

Peter Fjodorow[1] · Ortwin Hellmig[2] · Valery M. Baev[2]

Received: 30 January 2018 / Accepted: 21 March 2018 / Published online: 26 March 2018

Abstract
A broadband tunable Tm/Ho-doped fiber laser is developed for sensitive in situ measurements of intracavity absorption spectra in the spectral range of 4780–5560 cm^{-1}. This spectral range includes an atmospheric transmission window enabling sensitive measurements of various species. The spectral bandwidth of laser emission varies from 20 to 60 cm^{-1} and is well suitable for multicomponent spectroscopy. The sensitivity achieved in cw operation corresponds to an effective absorption path length of $L_{eff} = 20$ km, with a spectral noise of less than 1%. The spectroscopic system is applied for measurements of absorption spectra of H_2O, NH_3 and for simultaneous in situ detection of three isotopes of CO_2 in human breath, which is important for medical diagnostics procedures.

1 Introduction

Laser spectroscopic techniques aimed at sensitive detection of molecular absorption usually exploit the fundamental vibrational molecular transitions in the NIR or MIR spectral regions. This fact motivated a fast development of infrared laser sources for spectroscopic purposes during the last decades [1–3]. However, besides high sensitivity, many applications require simultaneous in situ multicomponent measurements in harsh environments, e.g., in human breath, gas discharges, flames, combustion engines or shock tubes. Furthermore, a time resolution in the µs region is often necessary to resolve the dynamics of the relevant processes. As a consequence, such demanding requirements can be fulfilled satisfactorily only by few spectroscopic techniques.

One of these techniques is the intracavity absorption spectroscopy (ICAS) [4]. The characteristic feature of ICAS is that the sample is placed inside the cavity of a broadband laser. Like in a multipass cell, the laser light completes many round trips through the absorber, ensuring a long effective absorption path, L_{eff}, i.e., high sensitivity. Broadband cavity losses, e.g., due to mirror transmission, optical distortions or scattering in the sample are compensated by the laser gain and do not influence the sensitivity of ICAS measurements. In contrast, the narrow line losses remain uncompensated and appear as absorption lines in the emission spectrum of the laser. To ensure proper performance of ICAS, the homogeneous line width of the gain has to be larger than the absorption line width of the sample. This requirement can be fulfilled with various lasers based on broadband gain media, such as dyes, crystals or glass fibers.

The absorption signal in the laser emission spectra with the ICAS technique is measured as the relative change of the spectral power density at the center of the absorption line. Consequently, fluctuations of the total power do not influence the sensitivity of these measurements. This feature is an important advantage of ICAS compared to other cavity-enhanced techniques, since it benefits in situ measurements in hostile environments [5, 6]. Another advantage of the ICAS technique is the capability of time-resolved analysis of transient processes by a broadband spectral recording [7]. Currently, the only competitive spectroscopic techniques enabling broadband, sensitive and time-resolved measurements in harsh environments are based on cavity-enhanced frequency comb spectroscopy [8, 9]. However, such techniques require expensive and technically complicated experimental setups, making the operation demanding and field

This article is part of the topical collection "Mid-infrared and THz Laser Sources and Applications" guest edited by Wei Ren, Paolo De Natale and Gerard Wysocki.

✉ Peter Fjodorow
peter.fjodorow@uni-due.de

[1] Institute for Combustion and Gas Dynamics-Reactive Fluids, University of Duisburg-Essen, Duisburg, Germany

[2] Institute of Laser Physics, University of Hamburg, Hamburg, Germany

applications difficult. In contrast, ICAS setups based on fiber lasers are easy to build and to operate [10].

In this paper, we demonstrate the first ICAS measurements carried out with a homemade broadband Tm/Ho-doped fiber laser operating in the spectral range 1.8–2.09 µm. The performance of the developed ICAS system based on a Tm/Ho fiber laser is demonstrated by applying it to sensitive measurements of NH_3-molecules at the ppb level, to the detection of atmospheric water vapor, and to simultaneous measurements of three stable isotopes of CO_2 in human breath.

Compared to a Tm-doped fiber laser (tunable from 1.7 to 1.98 µm) [11], the Tm/Ho laser is more favorable for practical measurements since its emission spectrum is extended toward longer wavelengths and includes an atmospheric transmission window enabling sensitive measurements of various species, such as N_2O, CH_4, NO, O_2, O_3, HCl, HBr and C_2H_2 [12]. Other solid state lasers applied for ICAS in this spectral region, e.g., Tm:YAG [13] and Co:MgF_2 [14] require a relatively low cavity loss and, therefore, cannot ensure measurements in hostile environments, e.g., in flames or in shock waves. In contrast, fiber lasers tolerate additional cavity losses of more than 20% without significant degradation of their performance and require a low pump power. Moreover, the spectral noise, which is naturally present in multimode lasers [15], can be easily reduced with fiber lasers by splicing a long piece of passive fiber to the active fiber, as demonstrated by monitoring single events in discharges and shock waves by broadband single-shot spectra [6, 7]. All these properties make fiber laser-based ICAS perfectly suitable for demanding spectroscopic applications in harsh environments.

2 Experimental setup

The experimental setup for our measurements is presented in Fig. 1. We use 30 cm of a Tm/Ho co-doped silica fiber (CorActive, TH550) with the following parameters: core/cladding diameters $d_{\mathrm{core/clad}} = 11.5/125$ µm, NA = 0.14 and $\lambda_{\mathrm{cutoff}} = 1.46$ µm. The weight fractions of the active ions are specified as 0.9% of thulium and 0.2% of holmium.

As a pump source, we use a laser diode (LD) emitting at 790 nm (Thorlabs, LD785-SH300), with a maximum power of 300 mW. The pump light is collimated with the lens L1 (Thorlabs, C230TME-B) and focused into the fiber core by the lens L2 (Thorlabs, C280TME-B). The homemade fiber coating M1 is a dielectric layer system, providing high transmission at 790 nm for the pump light and high reflectivity from 1.8 to 2.2 µm for the laser light. This coating acts as the end mirror of the resonator.

To avoid parasitic interferometric fringes, the second end of the fiber, and all other optical elements inside the laser

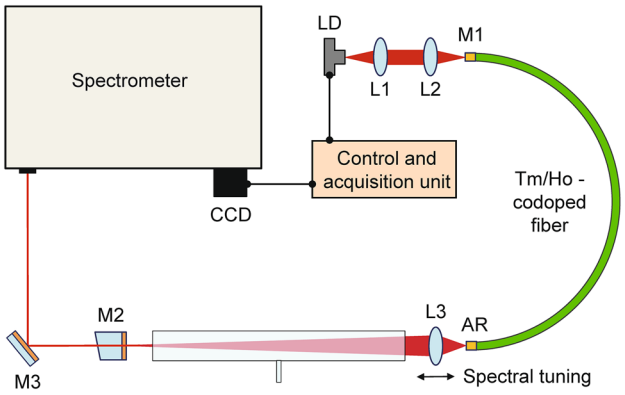

Fig. 1 Experimental setup

cavity, are anti-reflection (AR) coated. The lens L3 (Shott Hoya, A136) focuses the light coming from the fiber onto the plane output mirror M2 ($R \approx 98\%$) and back into the fiber again. Translation of the lens L3 along the optical axis leads to wavelength-dependent changes in the coupling efficiency due to chromatic aberration. The interplay between these added losses and the gain profile of the active fiber determines the position of the emission spectrum of the fiber laser. This is a very simple and effective method for wavelength tuning.

The laser light is coupled to a spectrometer (Jarell Ash 78-467, 1 m, 295 grooves/mm) and analyzed with a CCD line-scan camera (Goodrich Sensors Unlimited, SU-LDH, 1×1024 pixels). The total spectral resolution in the fourth order of diffraction is $\Delta\nu = 0.12$ cm^{-1}, corresponding to 3.6 GHz or $\Delta\lambda \approx 0.05$ nm at $\lambda = 2$ µm. The spectral calibration is performed by fitting the recorded absorption spectra of H_2O and CO_2 to the corresponding absorption spectra calculated from the HITRAN database [12], similar to the procedure used in previous experiments [5].

A sample gas probe is introduced into an open glass tube ($D = 1$ cm, $l = 40$ cm) placed between L3 and M2. The total optical length of the resonator is $L = 1$ m, providing a filling factor of the resonator with the absorber of $\beta = l/L = 0.4$.

The tuning range of the laser with atmospheric absorption is shown in Fig. 2. It is recorded by stepwise translation of the lens L3 in the first pulse of relaxation oscillations. For this purpose, the pump power is modulated above and below a threshold of about 50 mW, so that only one relaxation pulse appears. The accessible spectral region with this fiber laser is 4780–5560 cm^{-1} (1.8–2.09 nm). On the short wavelength side, it is limited by the mirror coating design and on the long wavelength side presumably by the low doping concentration of Ho ions. The individual spectra on the bottom of Fig. 2 correspond to different positions of the lens L3. Their spectral width of 20–60 cm^{-1} is well suitable for multicomponent spectroscopy.

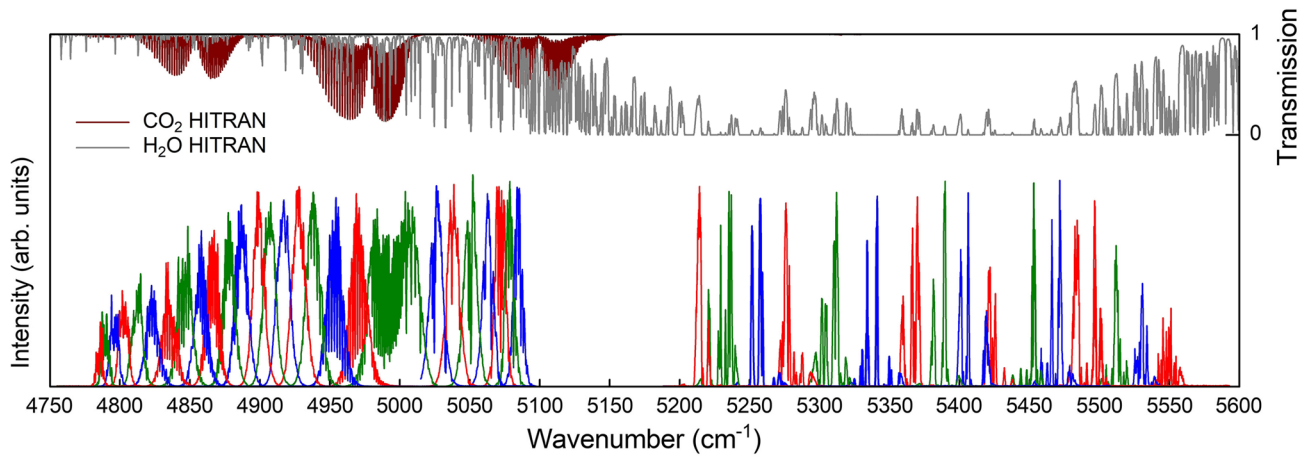

Fig. 2 Tuning range of the Tm/Ho fiber laser. Colored spectra (bottom) correspond to different positions of the lens L3. Simulated spectra (HITRAN) of atmospheric H_2O and CO_2 are shown on top

Atmospheric absorption spectra of H_2O and CO_2 simulated with the HITRAN database [12] for the absorption path length of 1 km are presented on the top. As can be seen, the atmospheric water vapor absorption is very strong in the spectral range of 5100–5550 cm^{-1} (1.8–1.96 µm). Since this spectral range has already been recorded previously with a Tm fiber laser [11], this experiment will be focused on the more advantageous region of 4780–5100 cm^{-1}.

The laser emission in the spectral range of 4780–5100 cm^{-1} is generated by Ho ions, whereas the emission in the range 5200–5560 cm^{-1} comes from Tm ions. In the intermediate spectral range from 5100 to 5200 cm^{-1} no laser action has been observed; however, simultaneous operation at 5090 and 5210 cm^{-1} is possible. Figure 3 shows that the relaxation oscillations of the fiber laser in both spectral ranges differ due to different ions participating in laser emission. In the intermediate spectral range, laser emission comes from Tm ions in the beginning and then from Ho ions.

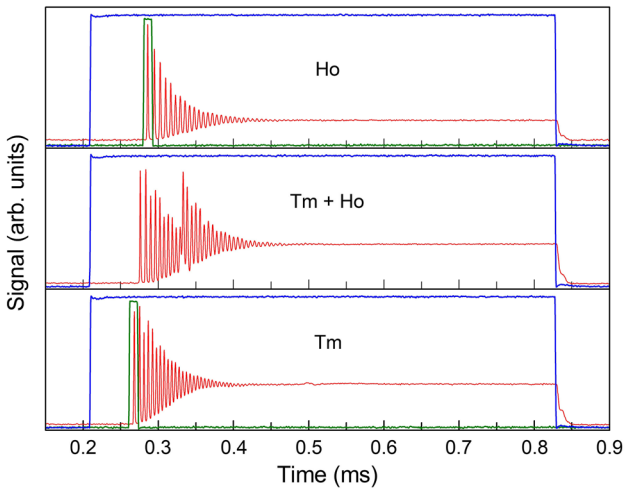

Fig. 3 Temporal behavior of the Tm/Ho fiber laser emission (red) recorded at 5050 cm^{-1} (top), at 5250 cm^{-1} (bottom) and under simultaneous operation in both spectral ranges (center), during modulation of the pump laser (blue). The detection window of the spectral recording (green) is adjusted to the first peak of relaxation oscillations

3 Sensitivity to intracavity absorption

The sensitivity of ICAS with a cw laser is determined by the spectral saturation time t_s [4], which depends upon laser parameters. However, if the duration of laser oscillation is short, $t < t_s$, the spectral sensitivity has the well-defined value

$$L_{\text{eff}} = c \times t, \tag{1}$$

with c being the velocity of light. In general, this permits us to adjust the sensitivity by the laser pulse duration and allows precise measurements of absorption coefficients and molecular concentrations.

In our experiment, we have estimated the sensitivity of the Tm/Ho fiber laser by recording the spectral dynamics of intracavity absorption signals, similar to the procedure reported earlier [16]. For that purpose, the laser emission spectrum is recorded at different relaxation pulses by adjusting the recording window of the CCD (green in Fig. 3). Figure 4 shows the emission spectra of the Tm/Ho laser recorded around 5065 cm^{-1} in different relaxation pulses.

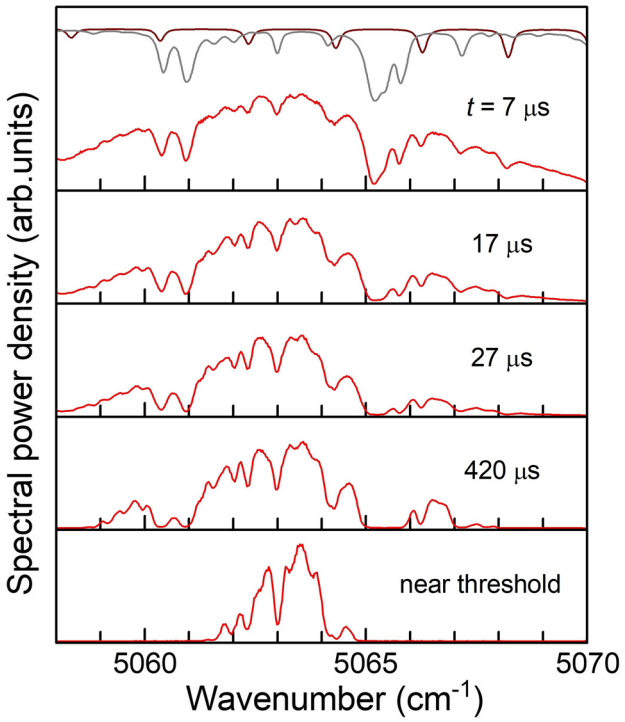

Fig. 4 Emission spectra of the Tm/Ho fiber laser (red) with intracavity atmospheric absorption of H_2O and CO_2 at different times after the onset of laser oscillation and in cw operation near threshold (bottom). Simulated atmospheric absorption spectra of H_2O (grey) and CO_2 (brown) are shown for comparison

Each of the presented spectra is averaged over 2000 laser pulses. Simulated atmospheric absorption spectra of H_2O and CO_2 (HITRAN) at the absorption path length of 1 km are shown in the upper diagram of Fig. 4 for comparison.

The temporal evolution of the laser emission shown in Fig. 4 demonstrates, that the absorption signals of water vapor absorption lines (e.g., at 5063 cm^{-1}) grow in the beginning and saturate at about $t_s = 30$ µs. According to Eq. (1), the spectral saturation time corresponds to the effective absorption path length of $L_{eff} = 9$ km (without taking into account the filling factor β, which can be made close to 1, if necessary). Higher sensitivity can be achieved by reducing nonlinear mode coupling in the laser when operating it near the threshold [4]. The bottom diagram of Fig. 4 shows, e.g., the emission spectrum of a cw laser at a low pump rate demonstrating the effective absorption path length of $L_{eff} = 20$ km, which was estimated by fitting spectra from the HITRAN database by varying the effective absorption path length and extrapolating the result to the case of $\beta = 1$. Since nonlinear mode coupling becomes relevant only at generation times of $t > t_s$, we have performed our measurements in the first relaxation pulse ($t < t_s$) to make accurate spectral measurements with a well-defined sensitivity independent of nonlinear effects. However, spectral recording with a higher sensitivity to intracavity absorption can be easily performed with a cw laser, if required.

4 Detection of NH_3

Sensitive detection of ammonia is very important, e.g., for atmospheric control and for clinical breath analysis [17, 18]. In our experiment, we demonstrate the possibility of sensitive ammonia detection in the cavity of a Tm/Ho fiber laser. Spectroscopic measurements are performed in the open intracavity cell (Fig. 1) at different partial flows of NH_3 within a constant NH_3/N_2 flow of 1000 sccm (standard cubic centimeter per minute) controlled by mass flow controllers (MKS, 1179B). The precise adjustment of small NH_3 concentrations in the total flow is achieved by diluting the partial flow of a 0.01% NH_3 in N_2 mixture (accurately prepared by Linde AG) with pure N_2. The laser operates in the first relaxation pulse and is tuned to the spectral range around 5045 cm^{-1}, where strong absorption lines of NH_3 are located. Figure 5 shows the recorded absorption spectra of NH_3 at partial flow rates ranging from 2 to 40 ppm.

The laser emission spectra in Fig. 5 recorded in the NH_3/N_2 flow (blue) are normalized by spectra recorded in a pure N_2 flow (grey). With this normalization, a substantial reduction of the technical spectral noise in the absorption spectra has been achieved. Furthermore, this procedure allows elimination of the atmospheric water vapor absorption lines (Fig. 5, red). The resulting spectra demonstrate a good agreement with the corresponding simulated HITRAN spectra of NH_3 (Fig. 5, green). The residual noise in the normalized spectra amounts to 0.6% (RMS).

The estimation of the detection limit for NH_3 is presented in Fig. 6. The minimal detectable concentration of NH_3 is determined by the extrapolation of the absorption signal of the strongest NH_3 line, located near 5046 cm^{-1}, to the noise level. With the Tm/Ho fiber laser being operated in the first pulse of relaxation oscillations and with the noise level of 0.6%, the detection limit of NH_3 is $p_{min,NH_3} = 60$ ppb. With a cw laser, NH_3 measurements in the low ppb range are possible. The detection of NH_3 in human breath in this spectral range is complicated due to interference of H_2O and CO_2 absorption lines. However, atmospheric measurements (as well as in other environments) of NH_3 can be performed with high sensitivity.

5 In situ detection of different CO_2 isotopes in human breath

Sensitive detection of different isotopes of various molecules is an important problem, e.g., for the detection of the bacterium *Helicobacter pylori* in human breath. This

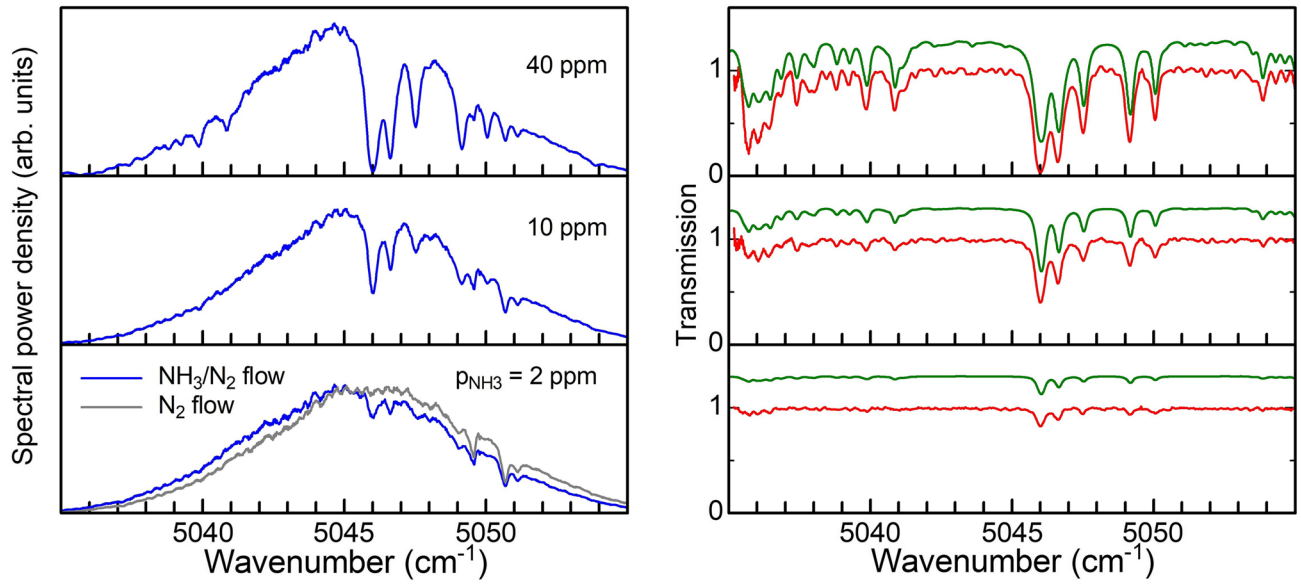

Fig. 5 Left: emission spectra of the Tm/Ho fiber laser with different partial flows of NH_3 in a 1000 sccm total flow of NH_3/N_2. A spectrum in a pure N_2 flow (grey in the bottom diagram) is recorded for normalization. Right: normalized experimental spectra (red) together with simulated HITRAN spectra of NH_3 (green)

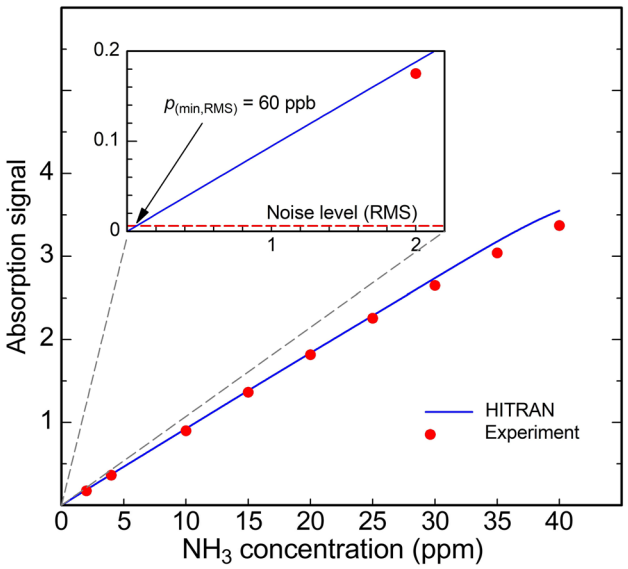

Fig. 6 Absorption signal of NH_3 at 5046 cm^{-1} derived from recorded experimental spectra (dots) and from simulated spectra (solid line) vs. NH_3 concentration. Inset: extrapolation of the HITRAN absorption signal (blue) to the noise level (red dashed line)

bacterium is often responsible for stomach ulcers, which can develop into cancer. The colonization degree of *H. pylori* can be determined by monitoring the $^{13}CO_2/^{12}CO_2$ isotope ratio in the exhaled breath [19]. Several spectroscopic techniques have been already used for breath analysis of $^{13}CO_2/^{12}CO_2$. However, usually these techniques require collection of the breath sample, performing some pre-treatment (drying, pre-concentration) and finally measuring the concentration in a clean environment, as, e.g., in the case of tunable diode laser absorption spectroscopy in the 2-µm region [20]. Recently, it has been shown that measurements of the isotope $^{16}O^{12}C^{18}O$ provide a higher diagnostic accuracy for the *H. pylori* [21]. Consequently, the established ^{13}C breath test could soon be replaced by this promising alternative. Besides that, the $^{16}O^{12}C^{18}O$ isotope has also been identified as a potential biomarker for diabetes [22]. Therefore, the development of sensitive and accurate detectors of the $^{16}O^{12}C^{18}O$ isotope is currently very important.

In our experiment, we perform in situ breath analysis in the laser cavity to demonstrate the possibilities of ICAS and, in particular, the promising capabilities of the Tm/Ho fiber laser system for the simultaneous in situ measurements of different isotopes of CO_2. During the experiment, the test person breathes out through a hose into the open glass tube placed inside the laser cavity. The laser is tuned to the spectral range around 4900 cm^{-1} and emits only the first pulse of laser relaxation oscillations. During an exhalation, an averaged spectrum, resulting from 2000 single shot spectra, is recorded within 200 ms. We performed these measurements in two overlapping spectral positions of the laser emission to analyze a broader spectral range and recorded atmospheric absorption spectra for normalization. The normalized spectra, combined into one single spectrum [5], are evaluated by fitting HITRAN spectra by varying the concentrations of CO_2 (natural mix) and H_2O.

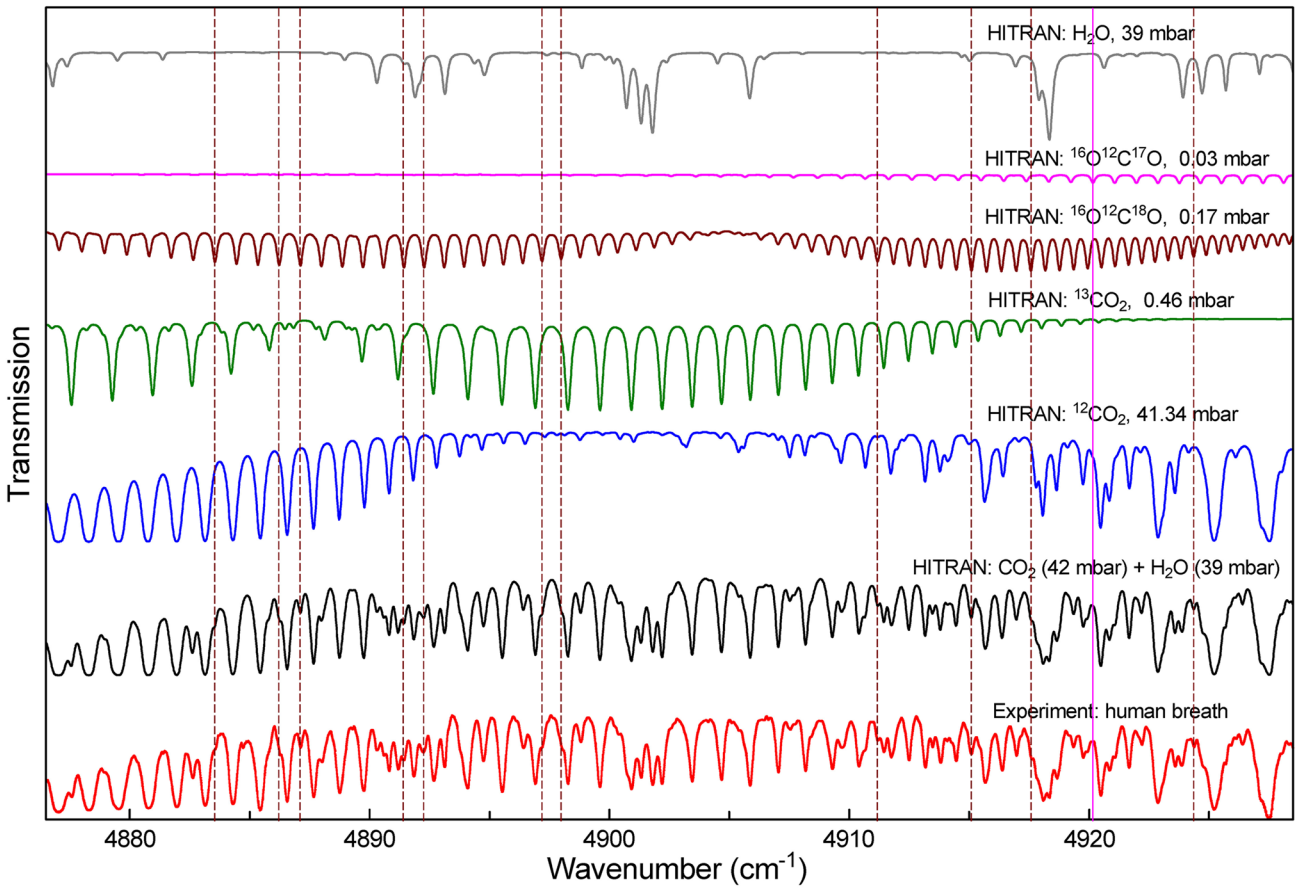

Fig. 7 The combined normalized spectrum of human exhalation in the cavity of a Tm/Ho fiber laser (red) shows good agreement with the best-fit HITRAN spectrum (black). Simulated spectra of H_2O and of different isotopes of CO_2 (natural ratio) are shifted along the vertical axis for better visualization. Dashed vertical lines show several absorption lines of the $^{16}O^{12}C^{18}O$-isotope, not overlapping with absorption lines of other species. The solid vertical line near 4920 cm^{-1} marks one absorption line, which can be used for the detection of the isotope $^{16}O^{12}C^{17}O$

The results are shown in Fig. 7, together with individual simulated spectra of H_2O and different CO_2 isotopes.

A comparison of the measured (red) and simulated spectra (black) shows an excellent agreement for all spectral features. The estimated breath concentrations of CO_2 and H_2O are 42 and 39 mbar, respectively. Furthermore, this comparison reveals that the natural ratio of CO_2 isotopes is preserved, as expected. It should be noted that the absorption lines of H_2O, $^{12}CO_2$, $^{13}CO_2$ and $^{16}O^{12}C^{18}O$ can be detected simultaneously. The dashed vertical lines indicate some absorption lines of $^{16}O^{12}C^{18}O$ that do not overlap with other species, and thus can be detected easily. Furthermore, the solid vertical line marks one isolated absorption line of the isotope $^{16}O^{12}C^{17}O$, which could also be detected with some additional effort. Note that although the concentrations of the presented CO_2 isotopes differ by several orders of magnitude, this spectral range is suitable for their simultaneous detection. The possibility to simultaneously monitor several absorption lines of each species using the Tm/Ho fiber laser ensures high accuracy in the determination of their concentrations, which is essential for medical diagnostics.

Since the determination of CO_2 isotope ratios is important not only for medicine, but also for, e.g., geology [23], mineralogy [24] and the exploration of other planets [25], our system is a promising tool for many practical applications.

6 Summary

In this paper, we present a broadband Tm/Ho fiber laser developed for sensitive absorption measurements inside the laser cavity. The laser is tunable in the spectral range of 5560–4780 cm^{-1} (1.8–2.09 µm) with the width of individual spectra varying within 20–60 cm^{-1}. The sensitivity of absorption measurements corresponds to the effective absorption path length of about 2 km in the first relaxation pulse to about 20 km in cw operation mode.

Table 1 Detection limits for species studied in this work

Species	Strongest line (cm^{-1})	Detection limit for L_{eff} = 800 m (ppb)	Detection limit for L_{eff} = 20 km (ppb)
H_2O	5413.90	50	2
NH_3	5046.02	100	4
$^{12}CO_2$	4989.93	880	35
$^{13}CO_2$	4899.61	1750	70
$^{16}O^{12}C^{18}O$	4915.17	2400	95
$^{16}O^{12}C^{17}O$	4951.18	2250	90

The values are calculated for the strongest absorption lines in the accessible spectral range of the Tm/Ho fiber laser, assuming a noise level of 1% and absorption path lengths of 800 m (third column) and 20 km (last column)

Our spectroscopic system is applied for measurements of absorption spectra of H_2O, NH_3 and for simultaneous in situ detection of three isotopes of CO_2 in human breath, which is important for medical diagnostics. The accessible detection limits for the investigated species, assuming a noise level of 1% and absorption path lengths of 800 m (corresponding to laser operation in the first pulse of relaxation oscillations and $\beta = 0.4$) and 20 km (corresponding to cw operation near threshold and $\beta = 1$), are summarized in Table 1.

These results demonstrate the possibilities of the developed system for sensitive multicomponent spectroscopy. The described ICAS system is a promising tool for a variety of challenging spectroscopic tasks. Besides the compact and monolithic experimental design, and the possibility to pump the Tm/Ho system with easily available laser diodes around 800 nm, a broad spectral range of 1.7–2.2 µm can be accessed with suitable design of mirror coatings and doping concentrations of thulium and holmium. As a result, a single spectroscopic system enables simultaneous detection of various species, e.g., H_2O, CO_2, N_2O, CH_4, NO, O_3, NH_3, HCl, HBr and C_2H_2, Furthermore, high tolerance to broadband losses and the accessible time resolution of about 100 µs make it possible to apply this detection system for broadband, sensitive and time-resolved measurements in harsh environments, e.g., in human breath, plasma, shock tubes or combustion engines.

References

1. M.W. Sigrist, R. Bartlome, D. Marinov, J.M. Rey, D.E. Vogler, H. Wächter, Trace gas monitoring with infrared laser-based detection schemes. Appl. Phys. B **90**, 289–300 (2008)
2. Y. Yao, A.J. Hoffman, C.F. Gmachl, Mid-infrared quantum cascade lasers. Nat. Photon. **6**, 432–439 (2012)
3. O. Henderson-Sapir, J. Munch, D.J. Ottaway, Mid-infrared fiber lasers at and beyond 3.5 µm using dual-wavelength pumping. Opt. Lett. **39**, 493–496 (2014)
4. V.M. Baev, T. Latz, P.E. Toschek, Laser intracavity absorption spectroscopy. Appl. Phys. B **69**, 171–202 (1999)
5. B. Löhden, S. Kuznetsova, K. Sengstock, V.M. Baev, A. Goldman, S. Cheskis, B. Pálsdóttir, Fiber laser intracavity absorption spectroscopy for in situ multicomponent gas analysis in the atmosphere and combustion environments. Appl. Phys. B **102**, 331–344 (2011)
6. P. Fjodorow, M. Fikri, C. Schulz, O. Hellmig, V.M. Baev, Time-resolved detection of temperature, concentration, and pressure in a shock tube by intracavity absorption spectroscopy. Appl. Phys. B **122**, 159 (2016). https://doi.org/10.1007/s00340-016-6434-8
7. P. Fjodorow, I. Baev, O. Hellmig, K. Sengstock, V.M. Baev, Sensitive, time-resolved, broadband spectroscopy of single transient processes. Appl. Phys. B **120**, 667 (2015). https://doi.org/10.1007/s00340-015-6181-2
8. A.J. Fleisher, B.J. Bjork, T.Q. Bui, K.C. Cossel, M. Okumura, J. Ye, Mid-infrared time-resolved frequency comb spectroscopy of transient free radicals. J. Phys. Chem. Lett. **5**(13), 2241–2246 (2014)
9. C. Abd Alrahman, A. Khodabakhsh, F.M. Schmidt, Z. Qu, A. Foltynowicz, Cavity-enhanced optical frequency comb spectroscopy of high-temperature H_2O in a flame. Opt. Express **22**, 13889 (2014)
10. P. Fjodorow, O. Hellmig, V.M. Baev, H.B. Levinsky, A.V. Mokhov, Intracavity absorption spectroscopy of formaldehyde from 6230 to 6420 cm^{-1}. Appl. Phys. B **123**, 147 (2017). https://doi.org/10.1007/s00340-017-6725-8
11. A. Stark, L. Correia, M. Teichmann, S. Salewski, C. Larsen, V.M. Baev, P.E. Toschek, Intracavity absorption spectroscopy with thulium-doped fibre laser. Opt. Commun. **215**, 113 (2003)
12. I.E. Gordon, L.S. Rothman, C. Hill, R.V. Kochanov, Y. Tan, P.F. Bernath, M. Birk, V. Boudon, A. Campargue, K.V. Chance, B.J. Drouin, J.-M. Flaud, R.R. Gamache, J.T. Hodges, D. Jacquemart, V.I. Perevalov, A. Perrin, K.P. Shine, M.-A.H. Smith, J. Tennyson, G.C. Toon, H. Tran, V.G. Tyuterev, A. Barbe, A.G. Császár, V.M. Devi, T. Furtenbache, J.J. Harrison, J.-M. Hartmann, A. Jolly, T.J. Johnson, T. Karman, I. Kleiner, A.A. Kyuberis, J. Loos, O.M. Lyulin, S.T. Massie, S.N. Mikhailenko, N. Moazzen-Ahmadi, H.S.P. Müller, O.V. Naumenko, A.V. Nikitin, O.L. Polyansky, M. Rey, M. Rotger, S.W. Sharpe, K. Sung, E. Starikov, S.A. Tashkun, J. Vande Auwera, G. Wagner, J. Wilzewski, P. Wcisło, S. Yu, E.J. Zak, The HITRAN2016 molecular spectroscopic database. J. Quant. Spectrosc. Radiat. Transf. **203**, 3–69 (2017)
13. J. Geng, J.I. Lunine, G.H. Atkinson, Absolute intensities and pressure-broadening coefficients of 2-mm CO_2 absorption features: intracavity laser spectroscopy. Appl. Opt. **40**(15), 2551–2560 (2001)
14. N.P. Vagin, A.A. Ionin, I.V. Kochetov, A.P. Napartovich, Y.P. Podmar'kov, M.P. Frolov, N.N. Yuryshev, Measurement of the O_2 ($b^1\Sigma_g^+ - a^1\Delta_g$) transition probability by the method of intracavity laser spectroscopy. Quant. Electron. **35**(4), 378–384 (2005)
15. V.M. Baev, G. Gaida, H. Schröder, P.E. Toschek, Quantum fluctuations of a multi-mode laser oscillator. Opt. Commun. **38**, 309–313 (1981)
16. J. Hunkemeier, R. Böhm, V.M. Baev, P.E. Toschek, Spectral dynamics of multimode Nd^{3+}- and Yb^{3+}-doped fibre lasers with intracavity absorption. Opt. Commun. **176**, 417–428 (2000)
17. E.V. Stepanov, Methods of highly sensitive gas analysis of molecular biomarkers in study of exhaled air. Phys. Wave Phenom. **15**, 149 (2007)
18. F.M. Schmidt, O. Vaittinen, M. Metsälä, M. Lehto, C. Forsblom, P.-H. Groop, L. Halonen, Ammonia in breath and emitted from skin. J. Breath Res. **7**, 017109 (2013)
19. A.S. Modak, Stable isotope breath tests in clinical medicine: a review. J. Breath Res. **1**, 104003 (2007)
20. S.N. Andreev, E.S. Mironchuk, I.V. Nikolaev, V.N. Ochkin, M.V. Spiridonov, S.N. Tskhai, High precision measurements of

the $^{13}CO_2/^{12}CO_2$ isotope ratio at atmospheric pressure in human breath using a 2 µm diode laser. Appl. Phys. B **104**, 73 (2011)
21. A. Maity, S. Som, C. Ghosh, G.D. Banik, S.B. Daschakraborty, S. Ghosh, S. Chaudhuri, M. Pradhan, Oxygen-18 stable isotope of exhaled breath CO_2 as a non-invasive marker of *Helicobacter pylori* infection. J. Anal. At. Spectrom. **29**, 2251–2255 (2014)
22. C. Ghosh, G.D. Banik, A. Maity, S. Som, A. Chakraborty, C. Selvan, S. Ghosh, S. Chowdhury, M. Pradhan, Oxygen-18 isotope of breath CO_2 linking to erythrocytes carbonic anhydrase activity: a biomarker for pre-diabetes and type 2 diabetes. Sci. Rep. **5**, 8137 (2015)
23. S. Guillon, E. Pili, P. Agrinier, Using a laser-based CO_2 carbon isotope analyser to investigate gas transfer in geological media. Appl. Phys. B **107**, 449 (2012)
24. D.J. Des Marais, J.G. Moore, Carbon and its isotopes in mid-oceanic basaltic glasses. Earth Planet. Sci. Lett. **69**, 43 (1984)
25. T.B. Sauke, J.F. Becker, Stable isotope laser spectrometer for exploration of Mars. Planet. Space Sci. **46**, 805 (1998)